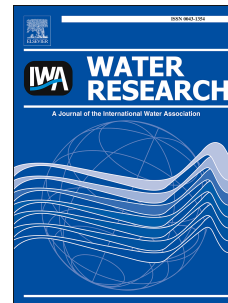


Accepted Manuscript

Identification of controlling factors for the initiation of corrosion of fresh concrete sewers

Guangming Jiang, Xiaoyan Sun, Jurg Keller, Philip L. Bond



PII: S0043-1354(15)00244-4

DOI: [10.1016/j.watres.2015.04.015](https://doi.org/10.1016/j.watres.2015.04.015)

Reference: WR 11244

To appear in: *Water Research*

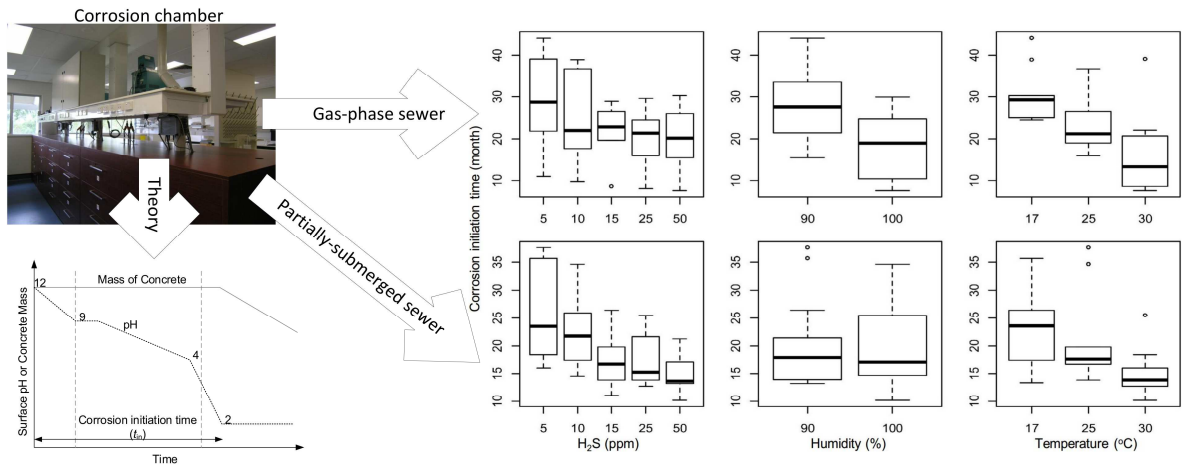
Received Date: 20 February 2015

Revised Date: 14 April 2015

Accepted Date: 15 April 2015

Please cite this article as: Jiang, G., Sun, X., Keller, J., Bond, P.L., Identification of controlling factors for the initiation of corrosion of fresh concrete sewers, *Water Research* (2015), doi: 10.1016/j.watres.2015.04.015.

This is a PDF file of an unedited manuscript that has been accepted for publication. As a service to our customers we are providing this early version of the manuscript. The manuscript will undergo copyediting, typesetting, and review of the resulting proof before it is published in its final form. Please note that during the production process errors may be discovered which could affect the content, and all legal disclaimers that apply to the journal pertain.



1 Identification of controlling factors for the initiation of corrosion 2 of fresh concrete sewers

3 Guangming Jiang¹, Xiaoyan Sun¹, Jurg Keller¹, Philip L. Bond^{1,*}

4 1. Advanced Water Management Centre, The University of Queensland, St. Lucia,
5 Queensland 4072, Australia

6 * Corresponding author. E-mail: p.bond@awmc.uq.edu.au, Tel.: +61 7 3365 4727; Fax: +61 7
7 3365 4726.

8 Abstract

9 The development of concrete corrosion in new sewer pipes undergoes an initiation process
10 before reaching an active corrosion stage. This initiation period is assumed to last several
11 months to years but the key factors affecting the process, and its duration, are not well
12 understood. This study is therefore focused on this initial stage of the corrosion process and
13 the effect of key environmental factors. Such knowledge is important for the effective
14 management of corrosion in new sewers, as every year of life extension of such systems has a
15 very high financial benefit. This long-term (4.5 year) study has been conducted in purpose-
16 built corrosion chambers that closely simulated the sewer environment, but with control of
17 three key environmental factors being hydrogen sulfide (H₂S) gas phase concentration,
18 relative humidity and air temperature. Fresh concrete coupons, cut from an industry-standard
19 sewer pipe, were exposed to the corrosive conditions in the chambers, both in the gas phase
20 and partially submerged in wastewater. A total of 36 exposure conditions were investigated to
21 determine the controlling factors by regular retrieval of concrete coupons for detailed analysis
22 of surface pH, sulfur compounds (elemental sulfur and sulfate) and concrete mass loss.

23 Corrosion initiation times were thus determined for different exposure conditions. It was
24 found that the corrosion initiation time of both gas-phase and partially-submerged coupons
25 was positively correlated with the gas phase H₂S concentration, but only at levels of 10 ppm
26 or below, indicating that sulfide oxidation rate rather than the H₂S concentration was the
27 limiting factor during the initiation stage. Relative humidity also played a role for the
28 corrosion initiation of the gas-phase coupons. However, the partially-submerged coupons
29 were not affected by humidity as these coupons were in direct contact with the sewage and
30 hence did have sufficient moisture to enable the microbial processes to proceed. The
31 corrosion initiation time was also shortened by higher gas temperature due to its positive
32 impact on reaction kinetics. These findings provide real opportunities for pro-active sewer
33 asset management with the aim to delay the on-set of the corrosion processes, and hence
34 extend the service life of sewers, through improved prediction and optimization capacity.

35

36 **Key words**

37 Sewer; corrosion; hydrogen sulfide; humidity; temperature; initiation time

38 **Nomenclature**

39	ANOVA	Analysis of variance
40	MAM	Minimum adequate model
41	MIC	Microbially induced corrosion
42	PLC	Programmable logic controller
43	SRB	Sulfate-reducing bacteria

- 44 SOB Sulfide-oxidizing bacteria
- 45 RH Relative humidity
- 46 RTD Resistance temperature detector
- 47

ACCEPTED MANUSCRIPT

48 **1 Introduction**

49 Existing sewers are valuable infrastructure and assets that have been established by
50 continuous public investment over the period of more than the past century. These sewers
51 have an estimated asset value of one trillion dollars in the USA (Brongers et al., 2002) and
52 \$100 billion in Australia. However, concrete corrosion is a costly deteriorating process
53 affecting sewer systems worldwide. Corrosion causes loss of concrete mass and structural
54 capacity, cracking of the sewer pipes and ultimately structural collapse. The rehabilitation
55 and replacement of damaged sewers involves very high costs. The sewer assets are being lost
56 at an estimated annual economic cost of around \$14 billion in USA alone (Brongers et al.,
57 2002) due to corrosion. This cost is expected to increase as the aging infrastructure continues
58 to fail (Sydney et al., 1996; US EPA, 1991).

59 Population growth and urbanization have led to continuous expansion of existing sewers and
60 replacement of outdated sewers. Fresh concrete sewer pipes and structures are installed
61 worldwide due to many advantages including low costs and flexibility. However, knowledge
62 about the development of corrosion on new concrete surfaces under sewer conditions is
63 limited. Gravity sewers offer favorable conditions for microbially induced corrosion, such as
64 available water (due to elevated relative humidity (RH)), high concentrations of carbon
65 dioxide, and high concentrations of H_2S (Wei et al., 2014). However, the fresh concrete
66 surface after construction is not suitable for microbial growth because of the high alkalinity.
67 Therefore, an initiation period is required to make the surface amenable for sulfide oxidizing
68 microorganisms.

69 The development of corrosion on concrete sewers can be divided into three stages, as shown
70 in Figure 1. During stage 1, the concrete surface is changed to a more favorable environment
71 for microorganisms due to carbonation and H_2S acidification (Islander et al., 1991; Joseph et

72 al., 2012). On the new concrete surface, owing to the presence of catalytic oxides, hydrogen
73 sulfide is chemically oxidized to sulfur in the form of very small crystals (Bagreev and
74 Bandosz, 2004; Bagreev and Bandosz, 2005). Overall, an important step is the dissociation of
75 hydrogen sulfide to HS^- in the adsorbed film of water on the concrete surface. This
76 dissociation is enhanced by the alkaline surface pH, which is an important factor for the
77 uptake of gaseous hydrogen sulfide during this first stage (Nielsen et al., 2006b). Additionally,
78 the chemical sulfide oxidation rate in the sewer is seen to double for a temperature increase of
79 9 °C by the same study. Therefore, relative humidity, H_2S concentration and temperature all
80 play a certain role in stage 1 of the corrosion development.

81 (Figure 1)

82 During stages 2 and 3, biological sulfide oxidation by netruophilic and acidiphilic sulfide
83 oxidising-bacteria will contribute to the sulfide oxidation to produce sulfuric acid (Cayford et
84 al., 2012; Okabe et al., 2007). This reacts with the cement material leading to the formation
85 of two important corrosion products: gypsum ($\text{CaSO}_4 \cdot 2\text{H}_2\text{O}$) in the matrix of the corrosion
86 layer and ettringite ($(\text{CaO})_3 \cdot \text{Al}_2\text{O}_3 \cdot (\text{CaSO}_4)_3 \cdot 32\text{H}_2\text{O}$) near the corrosion front where there is
87 higher pH (Jiang et al., 2014b; O'Connell et al., 2010). Recent studies show that the
88 biological sulfide oxidation rates correlate with H_2S concentration, relative humidity and
89 temperature (Jiang et al., 2014a; Nielsen et al., 2006a; Nielsen et al., 2005).

90 The total time span starting from fresh concrete surface to observed mass loss of concrete is
91 defined as the initiation time, i.e. t_{in} . It is clear that the length of initiation time depends on
92 many different factors due to the many processes and reactions involved. For a specific sewer
93 environment, it is beneficial to estimate t_{in} for the purpose of evaluating or optimizing current
94 corrosion prevention strategies. Although the well-known Pomeroy model can be used to
95 calculate the deterioration rate of concrete sewer pipes (Pomeroy, 1990), no model exists for

96 the estimation of t_{in} which is mainly due to the limited understanding of the controlling
97 factors for the corrosion initiation. Therefore, a full understanding of the relationship between
98 t_{in} and sewer environmental factors including H_2S concentration, relative humidity and
99 temperature is critical for the overall prediction of sewer corrosion.

100 This study aims to enhance understanding of the correlation between the initial development
101 of sewer corrosion and the sewer environmental factors including H_2S concentration, relative
102 humidity and temperature. In particular, to determine the controlling factors important for the
103 corrosion initiation time t_{in} . Fresh concrete coupons, either located in the gas-phase or
104 partially submerged in domestic wastewater, were exposed to thirty-six independent
105 conditions in well-controlled laboratory chambers that simulated conditions typically found
106 in various sewers, with six levels of H_2S concentration, two levels of relative humidity (RH)
107 and three levels of temperature. During the extended exposure experiment (over 4.5 years),
108 the change of surface properties, the formation of corrosion products and the mass losses due
109 to corrosion were measured regularly. The observed results were then statistically analyzed to
110 identify the controlling factors for the corrosion initiation time.

111 **2 Material and Methods**

112 **2.1 Concrete coupons**

113 The fresh concrete coupons were prepared from a new sewer pipe (1.2 m diameter \times 2.4 m
114 length and 0.07 m thickness) obtained from a sewer pipe manufacturer (HUMES, Sydney,
115 Australia). The HUMES concrete composition includes 10-20% Portland cement, about 60%
116 aggregates containing crystalline silica (quartz) sand, crushed stone and gravel, water at <20%
117 and other supplementary cementitious materials. Coupon dimensions were approximately 100
118 mm (length) \times 70 mm (width) \times 70 mm (thickness). After cutting, the coupons were washed

119 in fresh water to remove any surface contamination. Washed coupons were then dried in an
120 oven (Thermotec 2000, Contherm) at 60 °C for 3 days to achieve similar and stable initial
121 water content.

122 **(Figure 2)**

123 One of the original surfaces of the coupons, i.e. the internal surface of the pipe, was
124 designated as the surface to be exposed to H₂S. After cutting, the coupons were mounted in
125 stainless steel frames using epoxy (FGI R180 epoxy & H180 hardener) with the steel frame
126 providing a reference point for determining the change in thickness due to corrosion (Jiang et
127 al., 2014b). As described in section 2.2, the frame-enclosed coupons were used in the gas-
128 phase exposure. In addition, the same number of concrete coupons without enclosures were
129 partially submerged in real sewage in the corrosion chambers (Figure 3).

130 **2.2 Corrosion chamber and exposure condition**

131 Thirty-six identical corrosion chambers were constructed to achieve a controlled environment
132 simulating that of real sewers (Table 1). The controlled factors include combinations of three
133 gas-phase temperatures (17 °C, 25 °C and 30 °C), two levels of RH (100% and 90%) and six
134 H₂S levels (0 ppm, 5 ppm, 10 ppm, 15 ppm, 25 ppm and 50 ppm). The RH is sensitive to
135 temperature and the low RH (90%) fluctuated between 85% and 95%. Temperature and H₂S
136 variations are within 1 °C and 2 ppm, respectively.

137 **(Table 1)**

138 The chambers were constructed of glass panels of 4 mm thickness. The dimensions of the
139 chambers were 550 mm (L) × 450 mm (D) × 250 mm (H) (Figure 3). Each chamber
140 contained 2.5 L of domestic sewage that was collected from a local sewer pumping station
141 and replaced every two weeks. Seven coupons enclosed in frames were exposed to the gas

142 phase within the chambers with the exposed surface facing downwards approximately 110
143 mm above the sewage surface (Figure 3). This coupon arrangement simulated the sewer pipe
144 crown, a location which is reported to be highly susceptible to sulfide induced corrosion
145 (Mori et al., 1992; Vollertsen et al., 2008). Another six unmounted coupons were placed at
146 the bottom of the chambers. These were thus partially submerged (approx. 20-30 mm) in the
147 wastewater simulating the concrete sewer pipe near the water level, which is also a region of
148 high corrosion activity.

149 **(Figure 3)**

150 To achieve the specified H_2S gaseous concentrations in the corrosion chamber, Na_2S solution
151 was injected into a container partially filled with acid (13% HCl), using a corrosion-resistant
152 solenoid pump (Bio-chem Fluidics, model: 120SP2440-4TV) with a dispense volume of 40
153 μL . The H_2S concentrations were monitored using a H_2S gas detector (OdaLog Type 2) with
154 a range between 0 and 200 ppm (App-Tek International Pty Ltd, Brendale, Australia). A PLC
155 was employed to monitor the H_2S concentration and to trigger the dosing pump for Na_2S
156 addition to maintain the specified H_2S concentrations (Figure 3).

157 The corrosion chambers were installed in three cabinets, i.e. A, B and C (12 chambers each
158 cabinet), with different sewage temperatures controlled by re-circulating temperature
159 controlled water through glass tubes immersed in the sewage. The relative humidity was thus
160 controlled at approximately 100% or 90% for different chambers (Table 1). Humidity was
161 monitored using two resistance temperature detector (RTD) probes, of which one acts as wet
162 and another acts as dry bulb inside the chamber. Another of these probes was employed to
163 monitor the sewage temperature.

164 **2.3 Corrosion sampling and chemical analysis**

165 The corrosion chambers were operated for 54 months since December 2009. The
166 environmental factors were checked regularly to ensure the chambers being operated under
167 proper conditions. Periodically, at intervals between 6-10 months, one set of coupons (one
168 gas-phase coupon and one partially-submerged coupon) were retrieved from each corrosion
169 chamber for detailed analysis. A standard step-by-step procedure of various analysis was
170 employed to measure surface pH, followed by sampling for sulfur species (primarily
171 elemental sulfur and sulfate, as other sulfur compounds were found to be at nonsignificant
172 levels), and then photogrammetry analysis (thickness change).

173 A flat surface pH electrode (Extech PH150-C concrete pH kit, Extech Instruments, USA) was
174 used to measure the coupon surface pH. Steady pH readings were obtained after sufficient
175 contact between the pH probe and the coupon surface measuring spots that were wetted with
176 about 1 mL of milliQ water. Four measurements were made on randomly selected spots on
177 the coupon surface to determine an average value.

178 After measuring the surface pH, the exposed surface of concrete coupons was washed using a
179 high pressure washer (Karcher K 5.20 M). Four liter of water was used for each coupon. The
180 wash-off water was homogenized using a magnetic mixer for 2 hours before subsamples
181 taken into sulfide anti-oxidant buffer solution. A Dionex ICS-2000 IC with an AD25
182 absorbance (230 nm) and a DS6 heated conductivity detector (35 °C) was used to measure the
183 soluble sulfur species.

184 Five photos for each coupon were taken at different orientations to measure the coupon
185 thickness after washing using photogrammetry. A 3D image of the exposed surface for each
186 coupon was generated to calculate the surface height of the coupon relative to the stainless
187 steel frame as the reference plane. The decrease in thickness after certain exposure time was
188 then calculated by subtracting the average thickness after washing from the average thickness

189 before exposure. This technique not only enables an accurate change in coupon thickness to
190 be determined irrespective of the surface roughness but also provides a detailed record of the
191 spatial distribution of the losses that occurred.

192 **2.4 Data analysis**

193 As discussed, the concrete corrosion develops in three stages where in the third stage sulfuric
194 acid production occurs (Figure 1). Thus, we may define the corrosion initiation time, t_{in} , as
195 the time taken before detection of significant levels of sulfate on the concrete surface. Taking
196 into consideration the location of coupons and their actual sulfide oxidation rates, we
197 determined the critical levels of sulfate arbitrarily as 1 gS/m^2 and 10 gS/m^2 for the gas-phase
198 and partially-submerged concrete coupons respectively. Corrosion initiation time for all
199 coupons were then calculated as the time to reach the critical levels assuming a linear
200 increase of sulfate production with time. The estimated t_{in} was subsequently analyzed to
201 identify the controlling environmental factors of the corrosion initiation processes.

202 First, regression tree models (R ver 3.1.1, <http://www.R-project.org/>) were used to determine
203 which of the three environmental factors were important (exploratory analysis). Tree models
204 were used as they can give a clear picture of the structure in the data and they automatically
205 accommodate complex interactions between explanatory variables. Recursive partitioning,
206 that successively splits the data by the explanatory variables (i.e. H_2S concentration, relative
207 humidity and gas temperature), was used to distinguish groupings in the corrosion initiation
208 time. To further investigate the importance of each environmental factor for the corrosion
209 initiation, statistic models with all three factors were analyzed using analysis of variance
210 (ANOVA) in R. These maximal models were then simplified by backward selection to get
211 minimal adequate models (MAM).

212 **3 Results and Discussion**

213 3.1 Surface pH

214 For fresh coupons exposed to 0 ppm H₂S for 54 months there was little change in the surface
215 pH from an initial level of 10.6 (Figure 4). The only factor driving pH down on gas-phase
216 coupons exposed to 0 ppm of H₂S would be from CO₂, however, this could not cause further
217 decrease of the surface pH as the coupon surfaces had already reached an equilibrium with
218 regard to carbonation. Extended exposure in the H₂S free air at different temperatures and
219 humidity levels did not lower the pH significantly. Surface pH of partially-submerged
220 coupons exposed to 0 ppm of H₂S decreased slightly, within 1 unit, after 54 months of
221 exposure (Figure 4). This slight change could be attributed to the neutralization from CO₂ in
222 the gas, and other organic acids present in the wastewater.

223 (Figure 4)

224 Reduction of surface pH on other gas-phase coupons exposed to various H₂S concentrations
225 (5-50 ppm) was more significant due to the acidification by H₂S itself or its oxidation product,
226 i.e. sulfuric acid (Figure. SI-2). A trend of gradual decrease in surface pH with the time of
227 exposure is evident for gas-phase coupons exposed to H₂S. In general, higher H₂S
228 concentrations coincided with lower surface pH. The pH drop in the 100% RH chambers was
229 slightly more than that in 90% RH chambers. Likely, high humidity levels facilitated sulfide
230 oxidation, as pore water is essential for chemical reactions to occur in concrete and for the
231 development of the sulfide oxidizing microbial activities. In contrast to RH, there is no
232 discernable effects of temperature on the coupon surface pH drop.

233 For partially-submerged coupons the surface pH had lowered to about 4 for 5 ppm H₂S, with
234 some variations, after 54 months of exposure. The pH for coupons exposed to 10, 15, and 25
235 ppm H₂S was between 2 and 4 in the majority of the coupons. The partially submerged
236 coupons exposed to 50 ppm H₂S, had their surface pH reduced to around 2 for both the 100%

237 and 90% RH after 34 months of exposure. No discernable effects of RH and temperature
238 were observed on the coupon surface pH over time. Partially-submerged coupons were in
239 close proximity to water, and were consequently less sensitive to RH levels.

240 In comparison to gas-phase coupons, it is evident that the decrease of surface pH is more
241 prominent on partially-submerged coupons for all H₂S gas levels. This is partially due to the
242 different factors contributing to the overall pH reduction. At the initial stages, the surface pH
243 was lowered by H₂S and CO₂, which was facilitated by high moisture levels. This
244 acidification, as evident by high sulfide oxidation activities, started earlier on the partially
245 submerged coupons (Fig. SI-1 & SI-2).

246 Over time, the dominating trend was of acidification of the coupon surface. However, it was
247 noticed in a few cases after becoming acidic, the surface pH then increased somewhat. A
248 possible explanation for this is by oxidation of Ca(HS)₂, to form Ca(OH)₂, i.e. alkalinity, and
249 elemental sulfur. Another possibility is that during chamber maintenance and coupon
250 retrieval, the H₂S exposure was temporarily interrupted and alkalinity permeating from the
251 concrete causes this slight rise in surface pH.

252 **3.2 Sulfate and elemental sulfur**

253 Levels of elemental sulfur and sulfate on coupon surfaces clearly increased with the exposure
254 time and gaseous H₂S levels (Fig. SI-1 & SI-2). Both elemental sulfur and sulfate detected on
255 gas-phase coupons were limited, i.e. less than 40 gS/m². The difference of elemental sulfur
256 production on gas-phase coupons between the two RH conditions and three temperatures was
257 not clear. Although high levels of elemental sulfur, up to 40 gS/m² were detected, this was
258 about 10 times lower than the sulfate detected on the partially-submerged coupons (Fig. SI-2).
259 It is evident that the surface sulfate increases with increased gaseous H₂S levels and with
260 increased time of exposure. In the latest sampling events there were significantly higher

261 sulfate levels, implying very active sulfide oxidation, likely this resulting from the biological
262 processes being more active. No discernible differences were found for sulfate concentrations
263 between the two RH levels. For the partially submerged coupons at least, these would have
264 an increased moisture content as water would be drawn up from the submerged surface to the
265 corrosion layer, and thus overriding the effect of RH differences.

266 The first peak shown in the profiles of elemental sulfur without sulfate being present suggests
267 that the neutrophilic sulfide oxidizing microbes produce mainly elemental sulfur at the
268 corresponding intermediate pH levels. With the following decrease of surface pH, the
269 accumulated elemental sulfur was further oxidized to sulfate, probably by another group of
270 sulfide oxidizing microbes. At low pH, some elemental sulfur was detected on the coupon
271 surface (Figure SI-1). Likely this is due to elemental sulfur being a temporary intermediate of
272 sulfide oxidation, which is then finally oxidized to sulfate. The formation of elemental sulfur
273 is attributed to both chemical and biological sulfide oxidation (Okabe et al., 2007). It has also
274 been observed that S^0 can be temporarily stored in the corroding concrete layer when high
275 gaseous H_2S levels occur (Jensen et al., 2009; Sun et al., 2014).

276 As the concrete mass loss occurs by reactions with sulfuric acid, the percentage of sulfate
277 indicates the progress of the development of corrosion. Figure 5 shows evidently increasing
278 trend of sulfate percentage with exposure time, which is in accordance with the succession of
279 sulfide oxidizing microorganisms (Figure. 1). Partially-submerged coupons achieved 100%
280 of sulfide oxidation to sulfate for both 100% and 90% RH levels after 24 months of exposure.
281 However, the sulfate percentage on gas-phase coupons increased steadily with exposure time,
282 with higher levels attained for coupons exposed to 100% RH in comparison to 90% RH.

283 **(Figure 5)**

284 It was seen that the sulfate produced on gas-phase coupons at 90% RH was still lower than
285 the elemental sulfur, with the percentage as sulfate was most often less than 50% (Figure 5).
286 It is reported that for H₂S gas concentrations of between 5 and 50 ppm there is a surface pH
287 threshold of 8.3-9.4, that influences the extent of H₂S oxidation. Due to oxygen limitations in
288 the liquid film on the coupon surface, partial oxidation only occurs above the pH threshold,
289 and sulfate formation is only favored when the surface pH is below this threshold (Joseph et
290 al., 2012). For each of the H₂S levels above 5 ppm (10, 15, 25, and 50 ppm), the gas-phase
291 coupon surface pH has decreased to levels lower than the threshold (8.3-9.4) after nearly 3
292 years of exposure. The attenuating surface pH on those coupons would have led to the
293 complete oxidation of H₂S to form sulfate. Collectively, these observations confirmed that
294 gas-phase coupons are still in the early stage of corrosion: where a significant part of
295 acidification would mainly occur by H₂S.

296 Both gypsum (CaSO₄) and ettringite (Ca₆Al₂(SO₄)₃(OH)₁₂·26H₂O) can be formed in the
297 corrosion layer due to the production of sulfuric acid. Measured molar ratios between calcium
298 and sulfur (Ca:S) on the coupons were around 1.4 (0.8 – 2.5), which indicates the corrosion
299 products contain both gypsum and ettringite that have Ca:S molar ratios of 1 and 2
300 respectively. The high surface pH of the gas-phase coupons also favors the conversion of
301 gypsum into ettringite (Jiang et al., 2014b).

302 **3.3 Corrosion losses**

303 The thickness of gas-phase concrete coupons only started to decrease due to corrosion loss
304 after 34 months of exposure (Figure 6), reaching a maximum at the end of the exposure
305 period of 2-3 mm for high H₂S levels (25 and 50 ppm). These gas-phase coupons had a low
306 corrosion rate in this initial period. It is not evident that concrete coupons exposed to 100%
307 RH induced more corrosion losses than those under 90% RH, although higher sulfate was

308 detected for high RH coupons (Fig. SI-2). It is highly possible that higher levels of moisture
309 promote more active biological and or chemical sulfide oxidation, to produce higher
310 concentrations of sulfuric acid or elemental sulfur. However, the noticeable low levels of
311 sulfate detected on gas-phase coupons, in comparison to that on the partially-submerged
312 coupons, indicates that the corrosion is limited by the sulfide-oxidizing rate rather than H₂S
313 concentration.

314 **(Figure 6)**

315 In contrast, the corrosion loss of the partially-submerged concrete coupons had reached more
316 than 4 mm for those exposed to 25 and 50 ppm H₂S (Figure 6). This corresponds well to the
317 high measured sulfate levels on these coupons (Fig. SI-2). It is clear that corrosion losses are
318 directly correlated to H₂S concentrations (Figure 6). This suggests that H₂S is the decisive
319 factor for the corrosion rate, as reported before on pre-corroded concrete sewer (Jiang et al.,
320 2014a). This is in contrast to the gas-phase coupons, where it is likely that microbial activity
321 is the determining factor and hydrogen sulfide was not a limiting factor in this early stage of
322 corrosion initiation. Partially-submerged coupons are continuously inoculated and wetted
323 with wastewater in the corrosion chambers. Consequently, sulfide-oxidizing microbes might
324 be better developed on these coupons in comparison to the gas-phase coupons.

325 **3.4 Corrosion initiation time**

326 Corrosion initiation time, t_{in} , was determined for both gas-phase and partially-submerged
327 concrete coupons (Figure 7). For the gas-phase coupons t_{in} was more or less similar at 20
328 months for the different H₂S concentrations, except that of 5 ppm H₂S ($p=0.0079$, Table 2).
329 The expected trend of decreasing corrosion initiation time with increasing H₂S levels was not
330 evident. Instead, H₂S above 5 ppm seems to be a critical point for the t_{in} , implicating a certain
331 level of H₂S is required for significant corrosion development. This supports our findings of

332 corrosion losses on gas-phase coupons, which indicates corrosion is limited by the sulfide
333 oxidation rate, not the H₂S concentration (Section 3.3). For these gas-phase coupons it is
334 evident also that t_{in} decreases with higher temperature and higher humidity (Figure 7). Both
335 the Tree (Figure SI-3) and the ANOVA analyses (Table 2) were consistent with these
336 findings, emphasizing the importance of temperature and relative humidity on t_{in} , with
337 ANOVA p values of 5.95×10^{-6} and 6.86×10^{-7} for relative humidity and gas temperature,
338 respectively.

339 **(Figure 7)**

340 It is noticeable that for partially-submerged coupons the corrosion initiation time decreases
341 with increased H₂S concentration ($p=0.0044$). This confirms that H₂S is a key controlling
342 factor of the t_{in} over periods of long term exposure in sewer conditions. Temperature was
343 again shown to be a significant factor affecting the corrosion initiation time, with a p value of
344 0.0063. As found for the coupon surface sulfur compounds and corrosion losses (Section 3.2
345 and 3.3), the humidity was not a significant factor for t_{in} ($p=0.7459$). The data in Fig. 7 also
346 suggest that corrosion likely starts with the water line and reaches the crown gradually as
347 reported previously (Vollertsen et al., 2008). A minimum adequate model (MAM) was thus
348 identified through the backward selection processes which drops one explanatory factor for
349 the t_{in} each time. The MAM for gas-phase coupons includes all three experimental factors,
350 while the MAM for partially-submerged coupons only requires H₂S concentration and
351 temperature (Table 2).

352 **(Table 2)**

353 **3.5 Practical implications**

354 The observations of this study identified the controlling environmental parameters for the
355 initiation of corrosion on sewer concrete. The findings are relevant to develop strategies for

356 the prevention or reduction of sewer corrosion by prolonging the initiation time. One obvious
357 solution would be to reduce gaseous H₂S concentration, which could be achieved by dosing
358 sulfide sequestering agents or sewer biofilm controlling agents (Ganigue et al., 2011; Jiang et
359 al., 2013; Jiang et al., 2015; Jiang and Yuan, 2013; US EPA, 1974). However, it should be
360 noted that unless gaseous H₂S concentrations can be reduced down to below 5 ppm, the
361 corrosion initiation would still progress at the same pace for sewer crown areas (similar to the
362 gas-phase coupons in the corrosion chamber). It should also be noted that the corrosion
363 initiation time was only reduced from around 25 months at 50 ppm to 15 months at 5 ppm
364 (Figure 7), i.e. a 40% reduction of corrosion initiation time for a 90% reduction of H₂S
365 concentration. Also, liquid-phase technologies are not capable of reducing the relative
366 humidity in a sewer system. In contrast, sewer ventilation and gas treatment could be used to
367 decrease both H₂S and humidity, and consequently these would be more effective strategies
368 for prolonging the initiation of corrosion.

369 Another type of technology for preventing corrosion is by pipe relining or coating with
370 plastic or epoxy resins (Hewayde et al., 2007; Valix et al., 2012). These materials are more or
371 less inert to sulfuric acid. However, the coating material usually doesn't have alkaline
372 buffering capacity as fresh concrete, which means the surface can be easily inhabited by
373 acidiphilic sulfide-oxidizing bacteria due to the quick drop of surface pH. Consequently,
374 high concentrations of sulfuric acid will form on the sewer coating surface, which
375 inevitably will reduce the performance and life time of the coating. Other products might
376 provide such a sacrificial material like magnesium hydroxide, which will be eventually
377 exhausted but can slow down the corrosion development. It should be noted that the
378 corrosion initiation was largely due to the biological activity of sulfide oxidizing bacteria
379 enhancing sulfuric acid production. Pipe coating or relining materials that provide
380 antimicrobial properties and inhibit the microbial development on coating surfaces might be

381 the most useful strategies to ameliorate the damaging effects (Haile et al., 2010; Hashimoto,
382 2001). However, all corrosion reduction practice will lead to higher gaseous H₂S
383 concentration, potentially causes more odor problems.

384 **4 Conclusions**

385 The initiation of corrosion on fresh concrete surfaces in sewers was investigated in a 4.5-year
386 exposure study, which demonstrated that three elements were mainly affecting this process:

- 387 • Gas-phase H₂S concentration is an essential factor in initiating concrete corrosion
388 under sewer conditions. However, the corrosion is only limited by the H₂S supply at
389 concentrations at or below 10 ppm. At higher H₂S concentrations the sulfide oxidation
390 rate was the limiting factor during the initiation stage. This is contrary to the long-
391 term sulfide corrosion processes where even higher H₂S concentrations were still
392 increasing the corrosion rates.
- 393 • The corrosion initiation was positively correlated with the gas-phase temperature
394 mainly due to chemical reactions involved. This suggests a more rapid onset and
395 higher occurrence of sewer corrosion in warmer climates, and may be further
396 enhanced by ongoing climatic changes and increasing temperatures in urban areas.
- 397 • For concrete surfaces exposed to sewer air, humidity plays a significant role to
398 provide moisture to the concrete surface via vapor condensation. Moisture is
399 important for both the initiation and active corrosion stages. Ventilation can thus
400 delay the on-set and possibly mitigate against sewer corrosion through reduced
401 humidity.

402 **Acknowledgements**

403 The authors acknowledge the financial support provided by the Australian Research Council
404 and many members of the Australian water industry through LP0882016 the Sewer Corrosion
405 and Odour Research (SCORE) Project (www.score.org.au). Dr Guangming Jiang is the
406 recipient of a Queensland State Government's Early Career Accelerate Fellowship.

407 **References**

- 408 Bagreev, A. and Bandosz, T. (2004) Carbonaceous materials for gas phase desulphurization:
409 role of surface. *American Chemical Society, Division of Fuel Chemistry* 49(2), 817-821.
- 410 Bagreev, A. and Bandosz, T.J. (2005) On the Mechanism of Hydrogen Sulfide Removal from
411 Moist Air on Catalytic Carbonaceous Adsorbents. *Industrial & Engineering Chemistry*
412 *Research* 44(3), 530-538.
- 413 Brongers, M.P.H., Virmani, P.Y. and Payer, J.H. (2002) Drinking Water and Sewer Systems
414 in Corrosion Costs and Preventative Strategies in the United States, United States Department
415 of Transportation Federal Highway Administration.
- 416 Cayford, B.I., Dennis, P.G., Keller, J., Tyson, G.W. and Bond, P.L. (2012) High-throughput
417 amplicon sequencing reveals distinct communities within a corroding concrete sewer system.
418 *Applied and Environmental Microbiology* 78(19), 7160-7162.
- 419 Ganigue, R., Gutierrez, O., Rootsey, R. and Yuan, Z. (2011) Chemical dosing for sulfide
420 control in Australia: An industry survey. *Water Research* 45(19), 6564-6574.
- 421 Haile, T., Nakhla, G., Allouche, E. and Vaidya, S. (2010) Evaluation of the bactericidal
422 characteristics of nano-copper oxide or functionalized zeolite coating for bio-corrosion
423 control in concrete sewer pipes. *Corrosion Science* 52(1), 45-53.
- 424 Hashimoto, H. (2001) Evaluation of the anti-biofilm effect of a new anti-bacterial silver
425 citrate/lecithin coating in an in-vitro experimental system using a modified Robbins device.
426 *Kansenshogaku Zasshi* 75(8), 678-685.
- 427 Hewayde, E.H., Nakhla, G.F., Allouche, E.N. and Mohan, P.K. (2007) Beneficial impact of
428 coatings on biological generation of sulfide in concrete sewer pipes. *Structure and*
429 *Infrastructure Engineering* 3(3), 267 - 277.
- 430 Islander, R.L., Deviny, J.S., Mansfeld, F., Postyn, A. and Shih, H. (1991) Microbial Ecology
431 of Crown Corrosion in Sewers. *Journal of Environmental Engineering* 117(6), 751-770.
- 432 Jensen, H.S., Nielsen, A.H., Hvitved-Jacobsen, T. and Vollertsen, J. (2009) Modeling of
433 Hydrogen Sulfide Oxidation in Concrete Corrosion Products from Sewer Pipes. *Water*
434 *Environment Research* 81(4), 365-373.
- 435 Jiang, G., Keating, A., Corrie, S., O'Halloran, K., Nguyen, L. and Yuan, Z. (2013) Dosing
436 free nitrous acid for sulfide control in sewers: Results of field trials in Australia. *Water*
437 *Research* 47(13), 4331-4339.
- 438 Jiang, G., Keller, J. and Bond, P.L. (2014a) Determining the long-term effects of H₂S
439 concentration, relative humidity and air temperature on concrete sewer corrosion. *Water*
440 *Research* 65(0), 157-169.

- 441 Jiang, G., Sun, J., Sharma, K.R. and Yuan, Z. (2015) Corrosion and odor management in
442 sewer systems. *Current Opinion in Biotechnology* 33, 192-197.
- 443 Jiang, G., Wightman, E., Donose, B.C., Yuan, Z., Bond, P.L. and Keller, J. (2014b) The role
444 of iron in sulfide induced corrosion of sewer concrete. *Water Research* 49(0), 166-174.
- 445 Jiang, G. and Yuan, Z. (2013) Synergistic inactivation of anaerobic wastewater biofilm by
446 free nitrous acid and hydrogen peroxide. *Journal of Hazardous Materials* 250–251, 91-98.
- 447 Joseph, A.P., Keller, J., Bustamante, H. and Bond, P.L. (2012) Surface neutralization and
448 H₂S oxidation at early stages of sewer corrosion: Influence of temperature, relative humidity
449 and H₂S concentration. *Water Research* 46(13), 4235-4245.
- 450 Mori, T., Nonaka, T., Tazaki, K., Koga, M., Hikosaka, Y. and Noda, S. (1992) Interactions of
451 nutrients, moisture and pH on microbial corrosion of concrete sewer pipes. *Water Research*
452 26(1), 29-37.
- 453 Nielsen, A., m, H., Vollertsen, J. and Hvitved-Jacobsen, T. (2006a) Kinetics and
454 Stoichiometry of Aerobic Sulfide Oxidation in Wastewater from Sewers: Effects of pH and
455 Temperature. *Water Environment Research* 78, 275-283.
- 456 Nielsen, A.H., Hvitved-Jacobsen, T. and Vollertsen, J. (2005) Kinetics and stoichiometry of
457 sulfide oxidation by sewer biofilms. *Water Research* 39(17), 4119-4125.
- 458 Nielsen, A.H., Vollertsen, J. and Hvitved-Jacobsen, T. (2006b) Kinetics and stoichiometry of
459 aerobic sulfide oxidation in wastewater from sewers-effects of pH and temperature. *Water*
460 *Environment Research* 78(3), 275-283.
- 461 O'Connell, M., McNally, C. and Richardson, M.G. (2010) Biochemical attack on concrete in
462 wastewater applications: A state of the art review. *Cement & Concrete Composites* 32(7),
463 479-485.
- 464 Okabe, S., Odagiri, M., Ito, T. and Satoh, H. (2007) Succession of sulfur-oxidizing bacteria in
465 the microbial community on corroding concrete in sewer systems. *Applied and*
466 *Environmental Microbiology* 73(3), 971-980.
- 467 Pomeroy, R.D. (1990) *The Problem of Hydrogen Sulphide in Sewers*, Clay Pipe
468 Development Association Limited, London.
- 469 Sun, X., Jiang, G., L., B.P. and Keller, J. (2014) Impact of fluctuations in gaseous H₂S
470 concentrations on the sulfide uptake rate by concrete corrosion layers in sewers. *Water*
471 *Research* Submitted.
- 472 Sydney, R., Esfandi, E. and Surapaneni, S. (1996) Control concrete sewer corrosion via the
473 crown spray process. *Water Environment Research* 68(3), 338-347.
- 474 US EPA (1974) *Process design manual for sulfide control in sanitary sewer systems*.
- 475 US EPA (1991) *Hydrogen sulphide corrosion in wastewater collection and treatment system*
476 (Technical Report).
- 477 Valix, M., Zamri, D., Mineyama, H., Cheung, W.H., Shi, J. and Bustamante, H. (2012)
478 Microbiologically Induced Corrosion of Concrete and Protective Coatings in Gravity Sewers.
479 *Chinese Journal of Chemical Engineering* 20(3), 433-438.
- 480 Vollertsen, J., Nielsen, A.H., Jensen, H.S., Wium-Andersen, T. and Hvitved-Jacobsen, T.
481 (2008) Corrosion of concrete sewers-The kinetics of hydrogen sulfide oxidation. *Science of*
482 *the Total Environment* 394(1), 162-170.

483 Wei, S., Jiang, Z., Liu, H., Zhou, D. and Sanchez-Silva, M. (2014) Microbiologically induced
484 deterioration of concrete: a review. *Brazilian Journal of Microbiology* (ahead), 0-0.
485

ACCEPTED MANUSCRIPT

1

Table 1. Controlled environmental factors for the 36 corrosion chambers.

Chamber No.	Group [Gas temperature (°C)]					
	A [17 °C]		B [25 °C]		C [30 °C]	
	RH (%)	H ₂ S (ppmv)	RH (%)	H ₂ S (ppmv)	RH (%)	H ₂ S (ppmv)
1	90	0	90	0	90	0
2	100	0	100	0	100	0
3	90	5	90	5	90	5
4	100	5	100	5	100	5
5	90	10	90	10	90	10
6	100	10	100	10	100	10
7	90	15	90	15	90	15
8	100	15	100	15	100	15
9	90	25	90	25	90	25
10	100	25	100	25	100	25
11	90	50	90	50	90	50
12	100	50	100	50	100	50

2

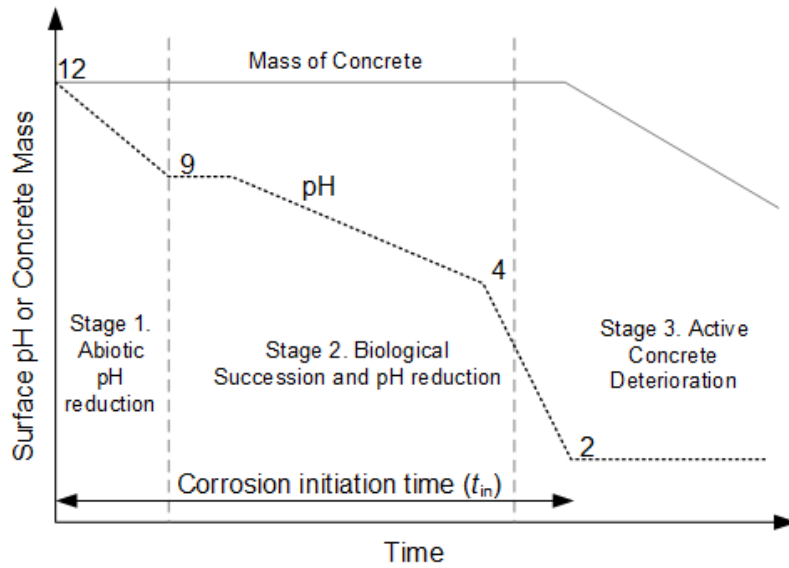
3

4 **Table 2.** Analysis of variance (ANOVA) for the corrosion initiation time (t_{in}) of gas-phase
5 concrete coupons.

		$t_{in} \sim H_2S + RH + T$ (Minimum adequate model)					
	Factors	¹ Df	Sum of Sq	RSS	F value	Pr(>F)	² Significance
Gas-phase concrete	H2S	1	195.5	810.9	8.2612	0.0079	**
	RH	1	758.0	1373.4	32.0282	5.95E-06	***
	T	1	1000.1	1615.4	42.2558	6.86E-07	***
		$t_{in} \sim H_2S + RH + T$					
Partially-submerged concrete	H2S	1	332.5	1223.1	9.7058	0.0044	**
	RH	1	3.7	894.3	0.1073	0.7459	
	T	1	302.4	1193.1	8.8289	0.0063	**
		$t_{in} \sim H_2S + T$ (Minimum adequate model)					
	H2S	1	332.5	1226.8	10.0377	0.0038	**
	T	1	302.4	1196.8	9.1308	0.0054	**

6 ¹ Df stands for degree of freedom; RSS, residual sum of square; Pr(>F), the p-value using the
7 F-test.

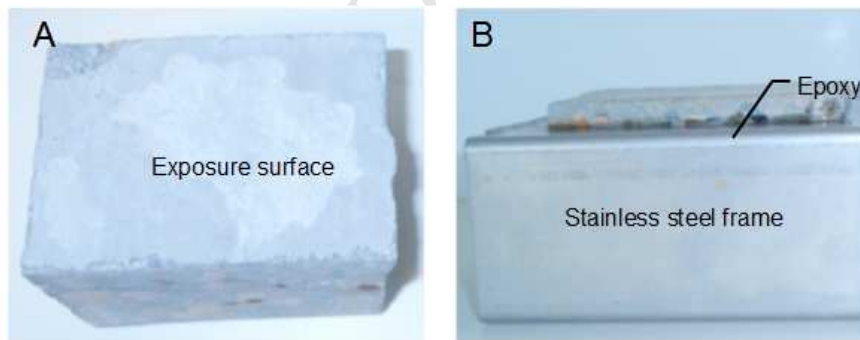
8 ² Significance codes based on the Pr value: 0-0.001: ***; 0.001-0.01: **; 0.01-0.05: *; 0.05-
9 0.1: .; 0.1-1: NA .



1

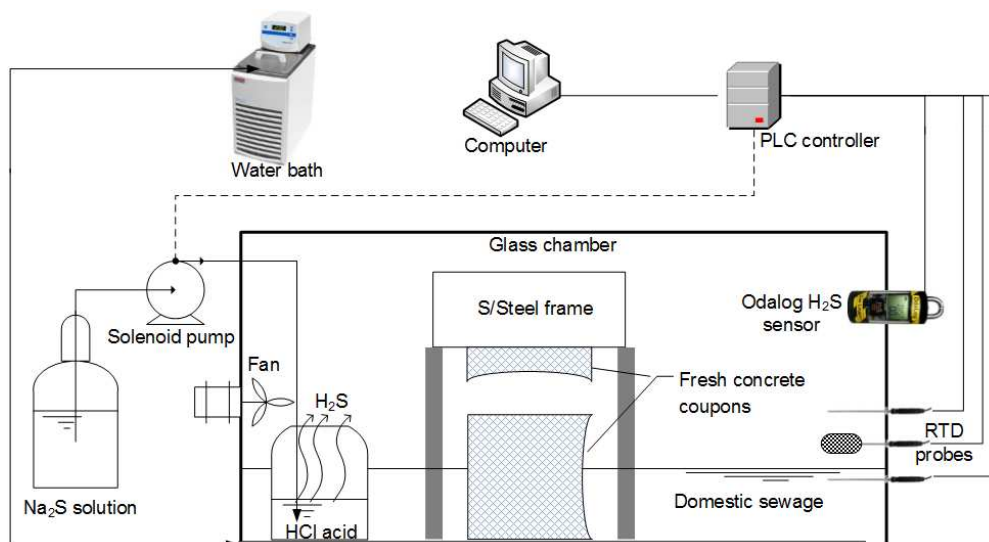
2 **Figure 1.** The development of microbially induced corrosion on new concrete sewer surfaces,
 3 adapted from Islander et al. (1991), with the corrosion initiation time (t_{in}) including stage 1, 2
 4 and a part of stage 3.

5



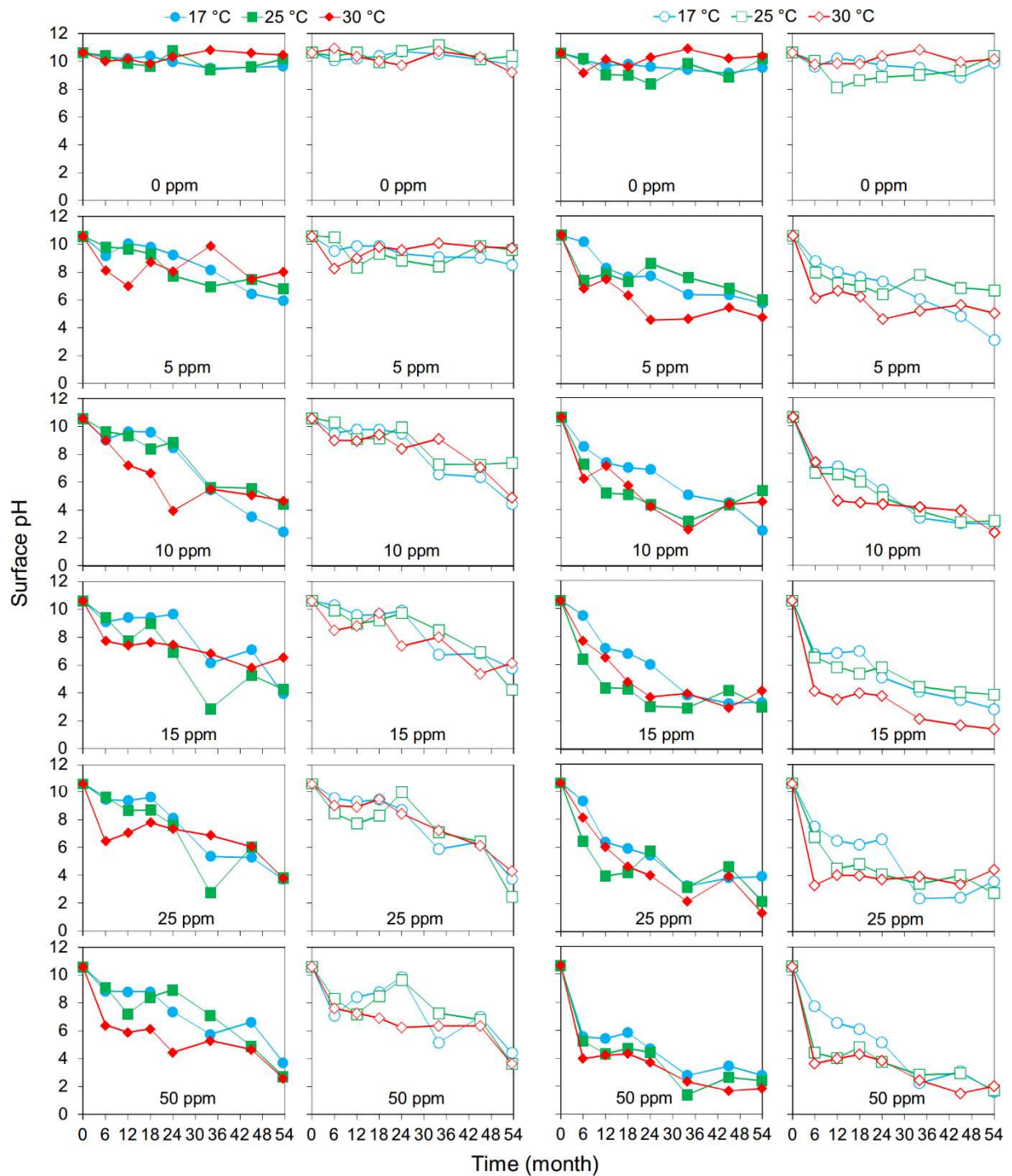
6

7 **Figure 2.** Photos of (A) a fresh concrete coupon; (B) the coupon mounted on a stainless steel
 8 frame with epoxy.



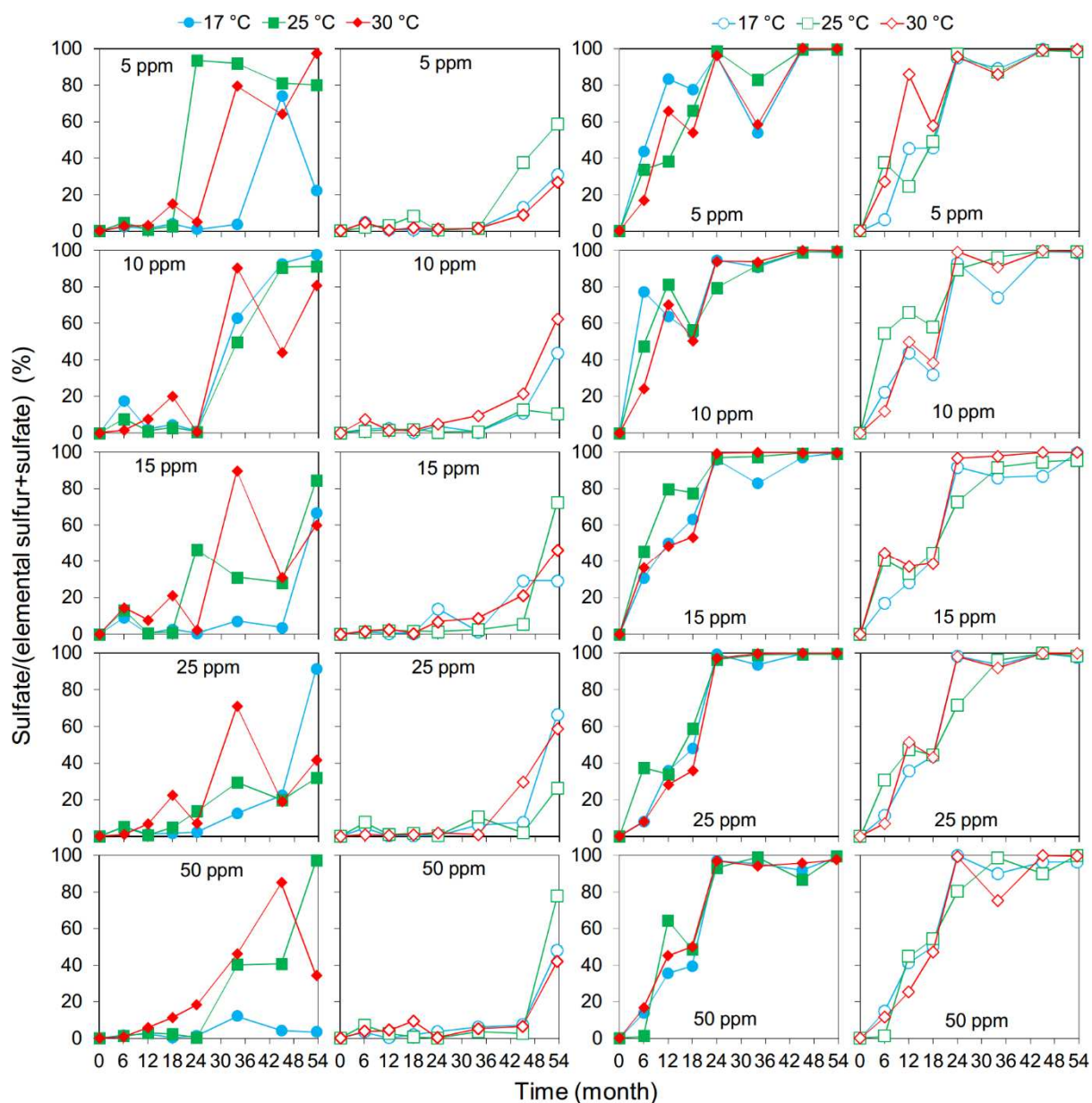
9

10 **Figure 3.** Side view of the corrosion chamber with H_2S concentration, relative humidity and
11 gas temperature controlled by programmable logic controller (PLC).



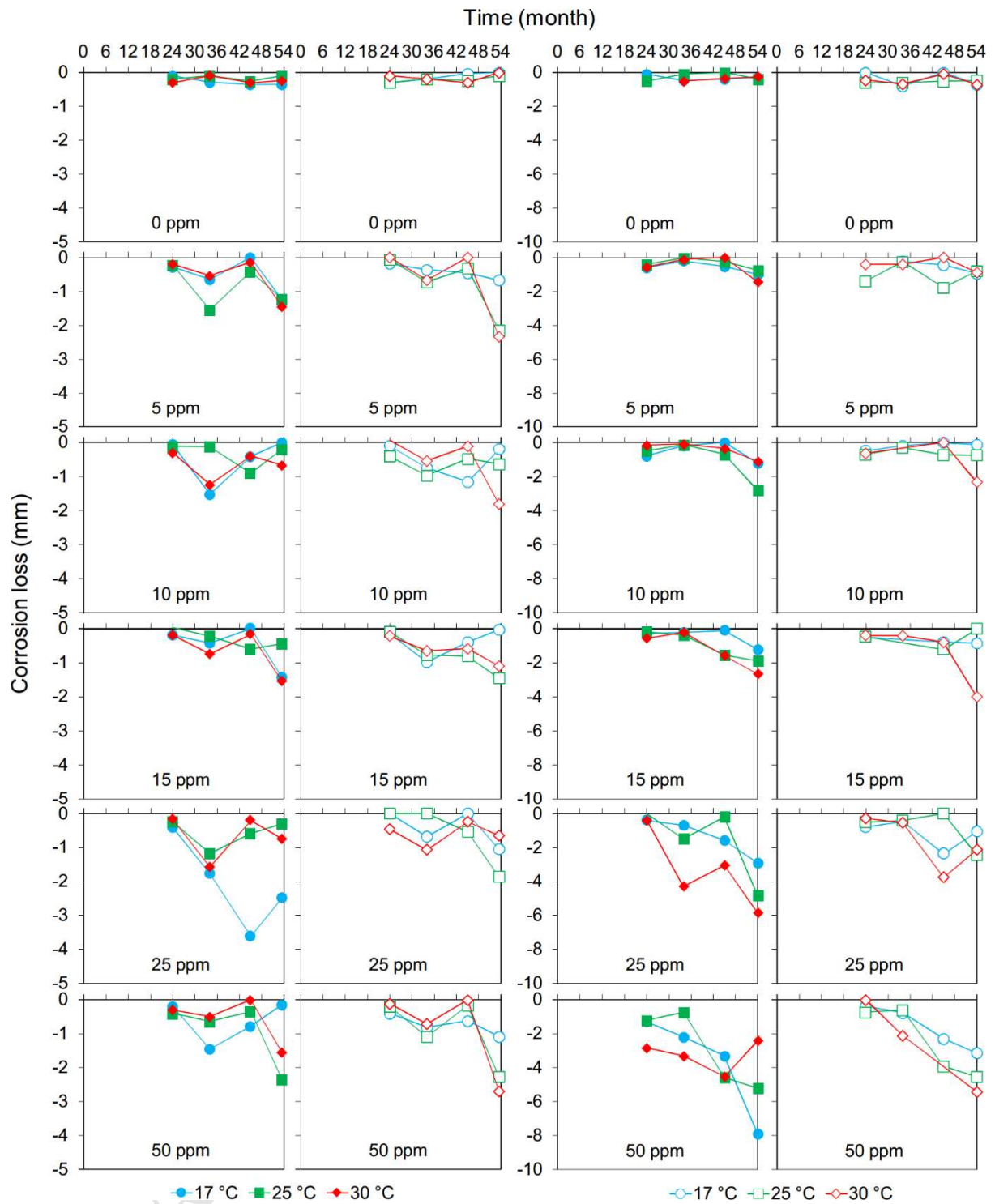
12

13 **Figure 4.** Surface pH of fresh concrete coupons exposed to different H₂S concentrations in
 14 corrosion chambers for 54 months. Plots in columns 1 & 2 and columns 3 & 4 are for
 15 coupons located in the gas-phase and those partially-submerged in sewage, respectively.
 16 Filled and empty symbols are for 100% and 90% relative humidity respectively.



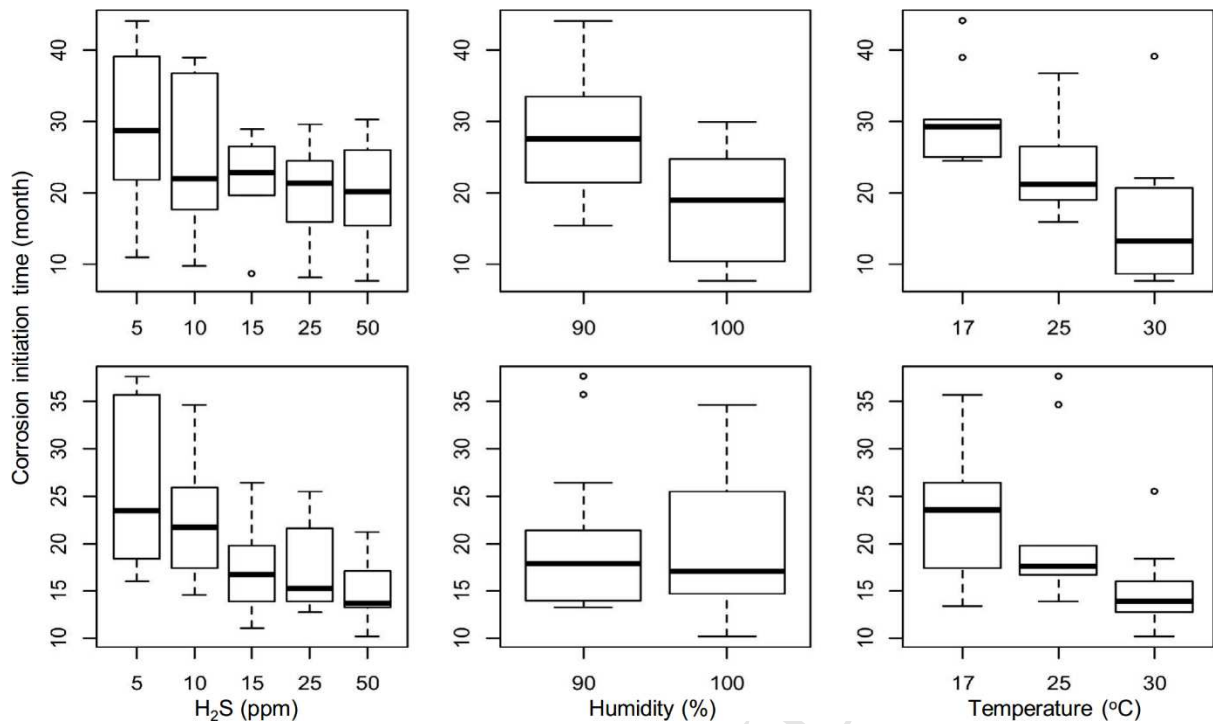
17

18 **Figure 5.** Percentage of sulfate as the final product of sulfide oxidation on the surface of
 19 fresh concrete coupons exposed to different H_2S concentrations in corrosion chambers for 54
 20 months. Plots in columns 1 & 2 and columns 3 & 4 are for coupons located in the gas-phase
 21 and those partially-submerged in sewage, respectively. Filled and empty symbols are for 100%
 22 and 90% relative humidity respectively.



23

24 **Figure 6.** Corrosion losses of fresh concrete coupons exposed to different H₂S concentrations
 25 in corrosion chambers for 54 months. Plots in columns 1 & 2 and columns 3 & 4 are for
 26 coupons located in the gas-phase and those partially-submerged in sewage respectively.
 27 Filled and empty symbols are for 100% and 90% relative humidity respectively.



Highlights

- A long-term study (4.5 years) focusing on the initiation of H₂S induced sewer corrosion
- The sulfide oxidation products gradually transform from elemental sulfur to sulfuric acid
- Corrosion initiation is controlled by H₂S only when the level is at or below 10 ppm
- Corrosion initiation is highly correlated with the gas temperature
- Humidity is important for the corrosion initiation on concrete exposed to air

Supplementary Information

Title: Identification of controlling factors for the corrosion initiation on concrete sewers

Authors: Guangming Jiang, Xiaoyan Sun, Jurg Keller, Philip L. Bond

Tables: 0

Graphs: 3

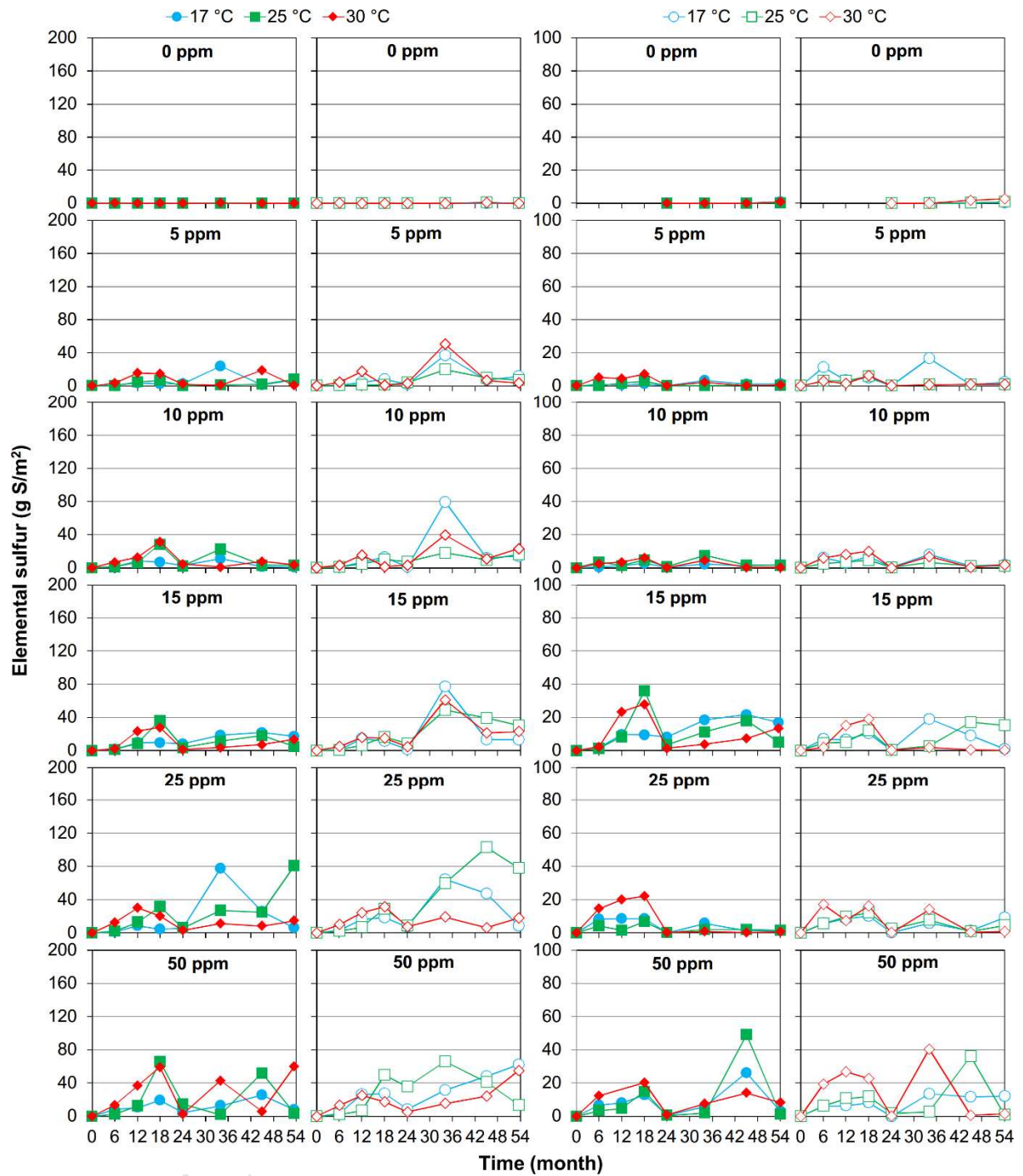


Figure SI-1. Elemental sulfur measured on the surface of fresh concrete coupons exposed to different H₂S levels in the corrosion chambers for 54 months. Plots in columns 1 & 2 and columns 3 & 4 are for coupons located in the gas-phase and those partially-submerged in sewage, respectively. Filled and empty symbols are for 100% and 90% relative humidity respectively.

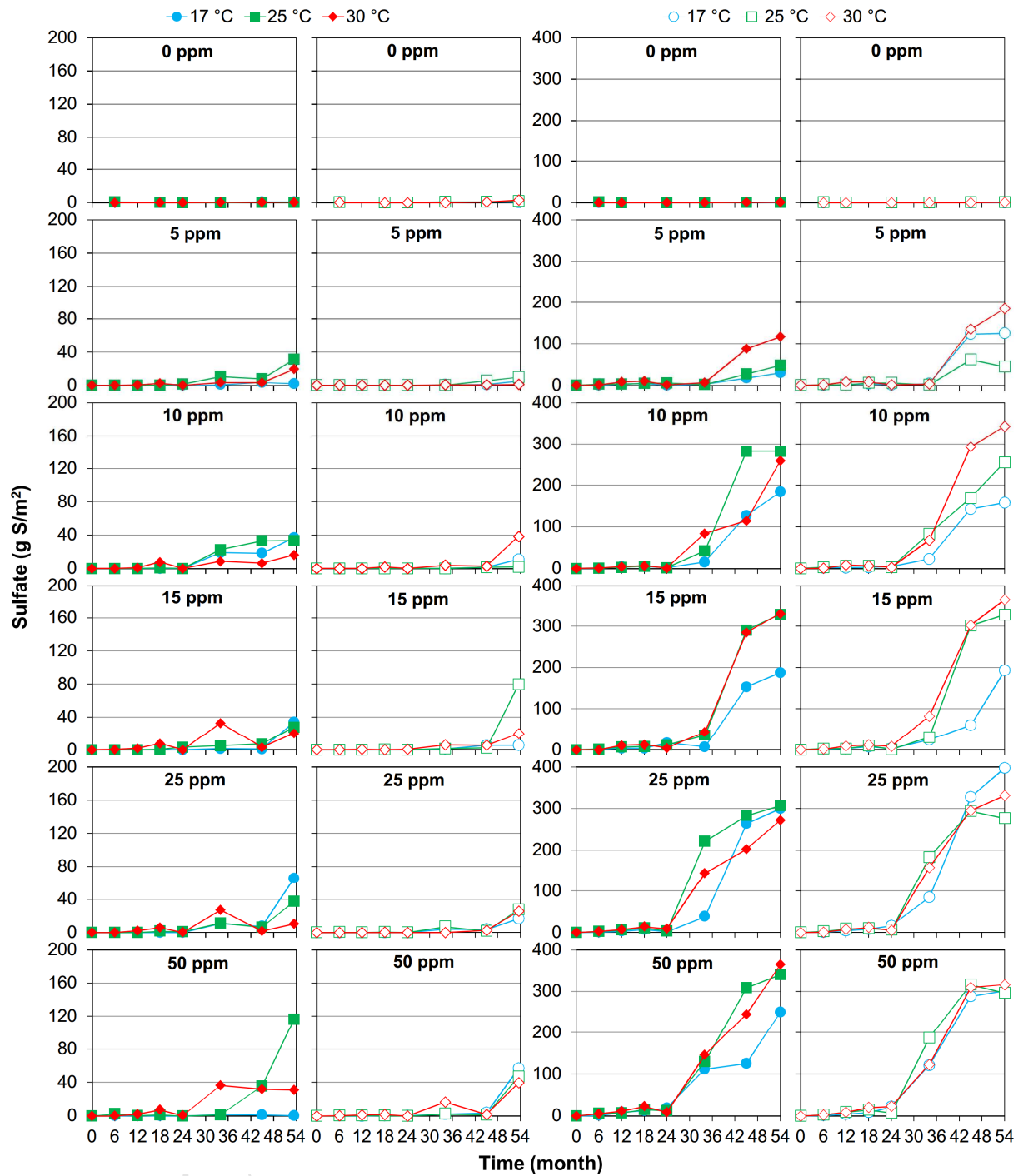


Figure SI-2. Sulfate measured on the surface of fresh concrete coupons exposed to different H₂S levels in the corrosion chambers for 54 months. Plots in columns 1 & 2 and columns 3 & 4 are for coupons located in the gas-phase and those partially-submerged in sewage, respectively. Filled and empty symbols are for 100% and 90% relative humidity respectively.

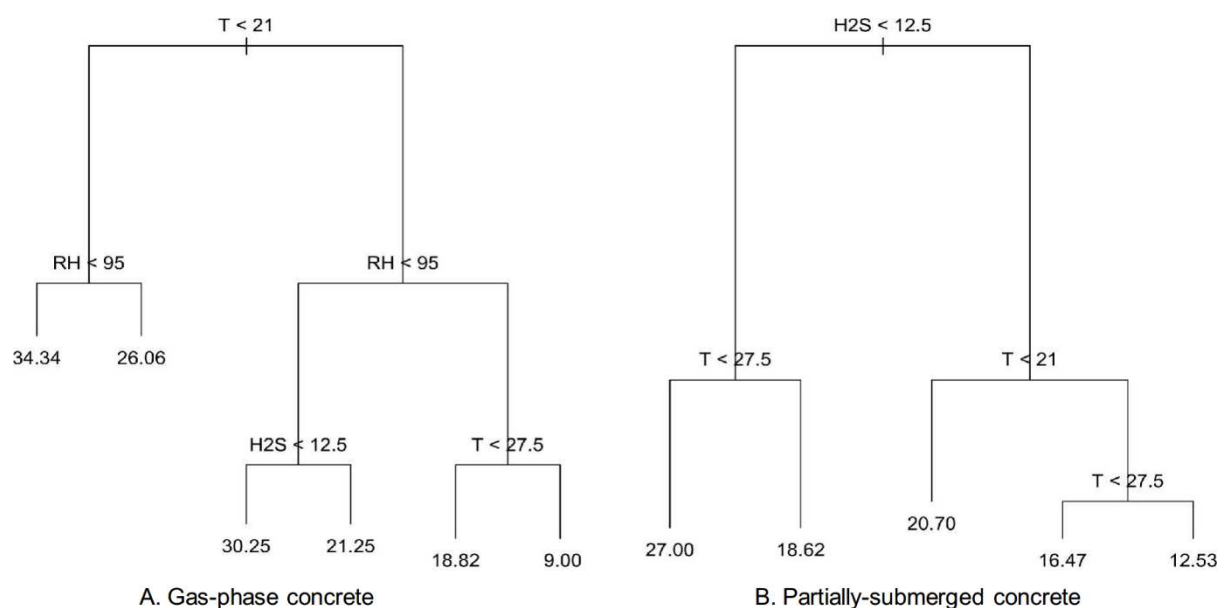


Figure SI-3. Trees for the corrosion initiation time of concrete coupons located in the gas-phase and those partially submerged in wastewater (from left to right). The expressions at each branch node are the splitting factor and the levels. E.g. $H_2S < 12.5$ means the corrosion rates can be partitioned into two groups by different H_2S levels. The left branch is the data for $H_2S < 12.5$ ppm and the right is for $H_2S \geq 12.5$ ppm. The numbers at the end of each branch are the mean values for the corrosion initiation time in that group. The analysis shows that different experimental factors contribute to the difference in the corrosion initiation time.